MAUSAM, **55**, 4 (October 2004), 611-624

551.510.42 : 504.06

Study of air quality at an industrial area in coastal India

ARUN KUMAR

Environment Management Department, Desein Pvt., Ltd., GK-II, Delhi, India

and

S. K. DASH

Centre for Atmospheric Sciences, Indian Institute of Technology, Delhi, India

(*Received 19 June 2002, Modified 2 February 2004*)

सार – भारत में विद्युत शक्ति के क्षेत्र में निजीकरण के बाद, देश की अर्थव्यवस्था के उदारीकरण में जीवाश्म–ईंधन–आधारित विद्युत उद्योगों की महत्वपूर्ण भूमिका है। प्रस्तावित विद्युत संयंत्रों के लिए चिमनी का डिज़ाइन तैयार करने और समुचित प्रदूषण – नियंत्रण के उपायों को अपनाने के लिए मॉडल तैयार किए जाने के प्रयासों से काफी सहायता मिलेगी । मौजूदा और प्रस्तावित प्रमुख उद्योगों से उत्सर्जित प्रदूषकों और विद्युत संयंत्रों के आस–पास की बस्तियों पर उनके दुष्प्रभाव के धरातल स्तर सांद्रण (जी. एल. सी.) का मूल्यांकन करने में डिस्पर्शन मॉडल का अल्पावधि (24 घंटे) उपयोग करते हुए इस मामले का अध्ययन किया गया है । नवीन डिज़ाइन डिस्पर्शन मॉडल (डी. डी. एम.) के परिणामों की तुलना अमेरिकी पर्यावरण संरक्षण अभिकरण के औद्योगिक स्रोत सम्मिश्र अल्पावधि (आई. एस. सी. एस. टी.) (वर्ज़न 3) मॉडल के परिणामों के साथ की गई है । डी. डी. एम. में रिफ्लेक्शन सहसंबद्ध टर्म का उपयोग जी. एल. सी. का परिकलन करने के लिए किया गया है । इसका लाभ यह रहा कि उस स्थान के समीप प्रदूषकों पर गुरुत्वीय तलछट के दुष्प्रभाव को भी इसमें शामिल किया जा सका । दोनों मॉडलों में पवन दिशा (डिग्री), पवन गति (ms^{-1}), तापमान (K), स्टेबिलिटि क्लास और मिश्रित ऊंचाई के घंटेवार मौसम आँकड़ों का इन्पुट के रुप में उपयोग किया गया है । खराब मौसम की स्थितियों के समय मानसून, मानसून पश्चात, ग्रीष्म और शीत ऋतु के दौरान प्रमुख उद्योगों से निकलने वाले SO_2 और NO_x की अल्पावधि जी. एल. सी. का पता लगाया गया है । प्रदूषण स्रोत के आस–पास के नौ स्थानों के सदृश प्रेक्षित मानों की तुलना SO_2 और NO_x के सांद्रणों का 8 घंटेवार मॉडल से किए गए पूर्वानुमान के साथ करने से यह संकेत मिलता है कि भारतीय परिस्थितियों के लिए आई. एस. सी. एस. टी. 3 मॉडल के परिणामों की अपेक्षा डी. डी. एम. के परिणाम अधिक उपयुक्त रहे ।

ABSTRACT. After privatization of the power sectors in India, the fossil-fuel-based power industries have an important role to play in the liberalization of the economy of the country. Modeling efforts will help a great deal in designing stacks and in taking appropriate pollution control measures for the proposed power plants. A case study has been cited with short-term (24-hour) use of dispersion model in assessing Ground Level Concentration (GLC) of the pollutants due to existing and proposed major industries, and their impact on large human settlement close to the power plants. The results of the new Desein Dispersion Model (DDM) are compared with those of Industrial Source Complex Short-Term, ISCST (version 3) model of the US Environment Protection Agency. In DDM, the reflection coefficient term has been used in calculating GLCs. This has the advantage of including the impact of gravitational settling on the pollutants close to the site. Hourly meteorological data of wind direction (degree), wind speed (ms^{-1}), temperature (K), stability class, and mixing height (m) have been used as input for both the models. Short-term GLCs of SO_2 and NO_x due to major industries have been assessed during monsoon, post-monsoon, summer and winter under worst meteorological conditions. Comparison of the 8 hourly model predicted concentrations of SO_2 and NO_x with the corresponding observed values at nine locations around the pollution source indicates that DDM results are more suitable for Indian conditions than those of ISCST3 model.

Key words – Ground level concentration, Coastal fumigation, Diurnal variation, Short-term impact, Model parameters.

1. Introduction

The meteorological conditions at a place play an important role in the transport, dispersion and deposition of air pollutants (Simpson, 1994). The meteorology at a location is a combination of weather peculiarities, *i.e.*, largescale (synoptic) flow, and mesoscale or local circulation systems, such as land and sea breezes, and topography features *i.e.*, anabatic or valley winds, and plain or plateau winds (Kurita *et al*., 1990; Savijarvi, 1995; Lu and Turco, 1994, 1995). Transport of air pollutants released by large industries situated at a coastal region are carried out by a secondary circulation system (Kurita *et al*., 1990 for the Tokyo Bay area; Wakimato and McEloy, 1986 for Los Angeles Basin; and Carroll and Baskett, 1979 for the San Francisco area). Dispersion and deposition are enhanced, when a neutral and unstable layer is capped with a stable or inversion layer over water creating a condition in which plume diffusion is large in the downwind direction over land. This produces high short-term (<1 hour) Ground Level Concentrations (GLC) due to coastal fumigation. The latter is due to the formation of Internal Boundary Layer (IBL) over land (Kambezidis *et al*., 1995). Increased GLCs of air pollution have adverse impact on life and economy. The nitrogen oxides (NO_x) are important air-pollutant components in understanding and modeling air pollution processes; they play a central role in atmospheric chemistry (Robert, 1990; Bower *et al*., 1994). NO_x function as catalyst in photochemical cycles by either producing or destroying ozone; they also generate nitric acid (HNO_3), an important constituent in acid precipitation, which damages vegetation and buildings (Khemani *et al*., 1989). These phenomena can result in human health impairment and phytotoxicity.

Power sectors have a key role in the liberalization of economy in India. Fast economic growth through industrialization may result in enhanced air pollution levels. A modeling exercise is needed to design stacks, and to identify steps needed for pollution control measures. The objectives of this paper are (*i*) to assess short-term GLCs of sulphur dioxide (SO_2) and NO_x due to existing and proposed industries during worst meteorological conditions, and (*ii*) to determine their impact on a large human settlement close to the site at Mangalore, on the Arabian Sea coast using hourly meteorological data in January, May, July and October 1996. It may be noted that in India the months of July and October represent active and post-monsoon phases of Indian Summer Monsoon, respectively. Further, one hour maximum impacts have been assessed due to existing and proposed sources under coastal fumigation. The study has been conducted using ISCST3 version 3 as well as a new model, named DDM. Sections 2.1 and 2.2 deal with the ICSCT and DDM models respectively. Similarities and differences between the two models, and the algorithm for coastal fumigation are discussed in Section 2.3. An overview of the parameters used in the model and description of the site are given in Section 3. Important results of the study are discussed in Section 4 and the conclusions are given in Section 5.

2. Description of dispersion models

2.1. *ISCST3 model*

In the ISCST3 model, U. S. EPA (1995), the origin of the coordinate system is considered to be at the ground, the base of the stack. The *x* - axis is taken positive along the downwind direction, the *y* - axis is normal to the *x* - axis, and the *z* - axis is in the vertical. The total hourly concentration, χ (x,y,z,t) for a steady state Gaussian plume**,** where t means time, is calculated on the combined source emissions as given below :

$$\chi(x,y,z,t)=\frac{QKVD}{2\pi U_s\sigma_y\sigma_z}\exp\left(-0.5\frac{y^2}{\sigma_y^2}\right) \qquad (1)$$

Here *Q*, *K*, *V* and *D* represent the pollutant emission rate (mass per unit time), the scaling coefficient to convert gs^{-1} into μgs^{-1}, vertical term for vertical distribution of the Gaussian plume and decay term $D = \exp(-\Psi\ x/U_s)$ accounts for the removal of pollutants by physical and chemical processes by the decay coefficient, $\Psi > 0$. It may be noted that the default value of $D = 1$ for $\Psi = 0$. σ_y and σ_z are the standard deviation of lateral and vertical concentration distribution (in meter) respectively. The mean wind speed (ms^{-1}) at stack height $U_s = U_{ref} (H/H_{ref})^p$, where U_{ref} is the reference velocity at height H_{ref} = 10 m above the ground and *H* is physical stack height. Wind profile exponent, *p*, is the function of stability class and wind speed.

Effects of gravitational settling and dry deposition on ambient concentration are neglected for gaseous pollutants and small sized particles (< 0.1 micron in diameter). The method of image source is used to account for multiple reflections from the ground and at the top of the mixing height. The effective plume height, H_e exceeds the mixing height, Z_i. Therefore, the GLC of the pollutant is zero. The following equation is used to calculate the vertical distribution of the plume without deposition :

$$V=\exp\left[-0.5\left(\frac{Z_r-H_e}{\sigma_z}\right)^2\right]+\exp\left[-0.5\left(\frac{Z_r+H_e}{\sigma_z}\right)^2\right]$$
$$+\sum_{i=1}^{\infty}\left\{\exp\left[-0.5\left(\frac{H_1}{\sigma_z}\right)^2\right]+\exp\left[-0.5\left(\frac{H_2}{\sigma_z}\right)^2\right]+\exp\left[-0.5\left(\frac{H_3}{\sigma_z}\right)^2\right]+\exp\left[-0.5\left(\frac{H_4}{\sigma_z}\right)^2\right]\right\}$$

Where,

$H_e = H + \Delta h$

$H_1 = Z_r - (2i\ Z_i - H_e)$

$H_2 = Z_r + (2i\ Z_i - H_e)$

$H_3 \;=\; Z_r \;-\; (2i\;\; Z_i + H_e)$

$H_4 \;=\; Z_r + (2i\;\; Z_i \;+ H_e)$

Here H and Δh are the physical stack height(m) and plume rise due to momentum and or buoyancy respectively. Similarly Z_r is the receptor height (m) above the ground and Z_i represents mixing height (m) respectively.

The infinite series term in the above equation accounts for the effect of limitation on the vertical plume expansion above the mixing layer. The vertical term within the surface mixing layer along the downwind direction is assumed rectangular instead of Gaussian. It indicates that there is a uniform concentration within the surface layer. V is defined by:

$$V = (2\pi)^{1/2}\left(\sigma_z Z_i^{-1}\right) \tag{2}$$

where $\sigma_z\ Z_i^{-1} \geq 1.6$. Eqn. 2 reduces the computational time and calculates V accurately. Buoyancy flux parameter F_b($m^4\ s^{-3}$) is calculated by :

$$F_b \;=\; g\ V_s\, d_s^2\ (\Delta T/4T_s) \tag{3}$$

where g (ms^{-2}) is the acceleration due to gravity, V_s (ms^{-1}) is the stack gas exit velocity, d_s(m) is the stack internal diameter at the top, ΔT is the difference between stack gas exit and ambient air temperatures, and T_s is the stack gas exit temperature. The cross over temperature, ΔT_c accounts for buoyancy and momentum dominated plume rise. If $\Delta T \geq \Delta T_c$, the plume rise is buoyancy dominated, otherwise it is momentum dominated. ΔT_c is calculated by the following expressions :

$$\Delta T_c = 0.00575\ \ T_s\,(V_s^{\,2/3}/d_s^{\,1/3}) \qquad F_b \;\geq\; 55\ (m^4\ s^{-3}) \tag{4}$$

$$\Delta T_c = \ 0.0297\ \ T_s\,(V_s^{\,1/3}/d_s^{\,2/3}) \qquad F_b \;<\; 55\ (m^4\ s^{-3})$$

H_e is estimated for unstable or neutral atmospheric conditions in terms of U_s and stack height, H (m), using the following expressions :

$$H_e \;=\; H + 38.71\ \ (F_b^{\,3/5}/\,U_s), \qquad F_b \geq\ 55\ (m^4\ s^{-3}) \tag{5}$$
$$H_e \;=\; H + 21.425\ (F_b^{\,3/5}/\,U_s), \qquad F_b <\ 55\ (m^4\ s^{-3})$$

The effective plume height, H_e, under stable atmospheric conditions is given by,

$$H_e = H + \left(2.6\frac{F_b}{U_s s}\right)^{1/3} \tag{6}$$

in terms of parameter, $s = \dfrac{g}{T}\dfrac{\partial\theta}{\partial z}$. Note that $\dfrac{\partial\theta}{\partial z}$ = 0.020 (km^{-1}) and the ambient temperature T for Pasquill stability classes E and F.

2.2. *Desein Dispersion Model (DDM)*

The mathematical expression of pollutant concentration, χ, at point (x,y,z) due to a steady point source averaged over time t, can be expressed in terms of downwind distance x, from the source, lateral distance y, vertical spread z, emission rate Q, wind speed at stack height U_s, dispersion coefficients σ_y and σ_z, representing lateral and vertical spreads respectively, as :

$$\chi(x,y,z,t) = \frac{Q}{2\pi U_s \sigma_y \sigma_z}\exp\left(-0.5\frac{y^2}{\sigma_y^2}\right)\exp\left(-0.5\frac{z^2}{\sigma_z^2}\right) \tag{7}$$

The reflection coefficient, r, is a measure of the amount of pollutant reflected from the ground. It is independent of meteorological conditions at the place of interest and does not account for resuspension or virtual point source calculation of the pollutants. It is assumed that pollutants hit the ground. Some of their amount may be deposited permanently and remainder is reflected. The pollutant reflected once from the ground has emission rates equal to rQ for the first reflection and equal to r^2Q and so on for the subsequent reflections. The potential value of reflection coefficient (Dumbauld *et al*., 1976 ; Bowers *et al*., 1979) is given by :

$$r \;=\; 0.75 - 2.5\, v$$

where, v (ms^{-1}) is the settling speed. It accounts for the particles settled under gravity or gases scavenged by vegetation and is in the range $0.04 < v < 0.3$. It is assumed that settling in turbulent planetary boundary layer occurs in average at the same rate as in a non-turbulent one. Pollutant concentration (Eqn. 7) at a point (x,y,0) on the ground (z = 0) is therefore :

$$\chi(x,y,0,t) = \frac{(1+r)Q}{2\pi U_s \sigma_y \sigma_z}\exp\left(-0.5\frac{y^2}{\sigma_y^2}\right)\exp\left(-0.5\frac{H_e^2}{\sigma_z^2}\right) \tag{8}$$

Here, z represents H_e with source on the ground (z = 0). Mixing height (Z_i) is being introduced in the model to account for pollutant concentration under the condition, $Z_i > H_e$. Eqn. (8) can, therefore, be written as :

$$\chi(x,y,0,t) = \frac{(1+r)Q}{2\pi U_s \sigma_y \sigma_z} \exp\left(-0.5\frac{y^2}{\sigma_y^2}\right)\left[\exp\left(-0.5\frac{H_e^2}{\sigma_z^2}\right) + \sum_{n=1}^{\infty} r^{(n-1)}\left\{\exp\left(-0.5\frac{(2nZ_i - H_e)^2}{\sigma_z^2}\right) + r\exp\left(-0.5\frac{(2nZ_i + H_e)^2}{\sigma_z^2}\right)\right\}\right] \quad (9)$$

It is assumed that when the H_e exceeds the inversion base ($H_e > Z_i$), pollutant GLCs are zero.

2.3. *Comparison of ISCST3 and DDM*

Both ISCST3 and DDM are based on Gaussian plume dispersion equation used for point sources with hourly values of wind speed (ms^{-1}), wind direction (degrees), temperature (K), stability class and mixing height (m) as input. The same model parameters are used in a 10 km radius around the proposed site, since the advection effect dominates over diffusion for large distances. The hourly mixing height values for a rural area for all stability categories is used in both models as the proposed site satisfies the criteria of Central Pollution Control Board (CPCB), 1997-98 for rural areas.

In the ISCST3 model, the vertical term is used without deposition. Gravitational settling and dry deposition of the gaseous small sized pollutants (< 0.1 micron in diameter) are neglected. The method of image sources is used to account for multiple reflections of the plume from the ground and the top of the mixing height. On the other hand, in DDM, a term, known as reflection coefficient, is being utilized which gives the fraction of pollutant amount reflected from the ground many times. Reflection of plume from the ground results in increase of GLC which is higher during unstable atmospheric conditions. DDM considers these boundary effects by the introduction of image sources (2nd and 3rd terms in Eqn. 9). The reflection coefficient depends on the settling velocity and is independent of meteorological conditions at the locality. The dependence of reflection coefficient on the kind of vegetation, season, time of the day, humidity, soil moisture and degree of turbulence has not been included in the model. The vertical variation of wind speeds are computed at the stack height. Nonlinear variation of wind speeds are not considered in the algorithm.

As the rising sun heats the surface, the neutral or unstable surface layer increases in height and gradually reaches the stack top. The plume initially emitted into a stable layer is afterwards enveloped by neutral or unstable air resulting in high GLC (χ_i) within a short distance

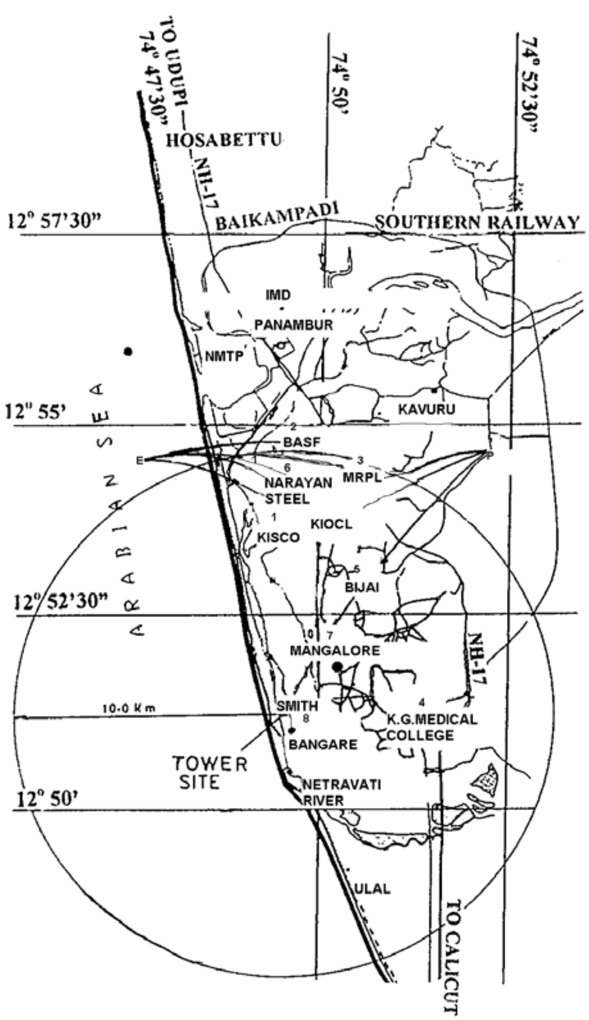

Fig. 1. Location of the existing and proposed industries marked by letters E and P respectively and nearby human settlements. Location numbers from 1 to 9 where pollutant concentrations are considered represent Baikampadi, Bala, Hosabettu, Jokatte, Kalavar, Kolambe, Konchade, Kavoor, Panambur respectively

(~1 km) from the stack over a period of less than 1 hour. It is assumed that no pollutant enters the inversion layer. The horizontal distribution of the plume is Gaussian type, and the vertical distribution is constant at a particular location (Stunder and SethuRaman, 1986) within the surface mixing layer. The horizontal and vertical diffusions, σ_{yi} and σ_{zi}, calculated for a rural area at a distance 100 m < x < 10000 m and stability class B (CPCB, 1997 - 98) are given by :

$$\sigma_{yi} = 0.16\ x\,(1 + 0.0001\ x)^{-0.5} \quad (10a)$$

$$\sigma_{zi} = 0.12\ x \quad (10b)$$

TABLE 1

Stack characteristics and emission data of major industries

Status of sources	Major industries	Receptor Location (x,y) in meter	Emission ($g\ s^{-1}$)		d_s	H	T_s	V_s
			SO_2	NO_x	(m)	(m)	(K)	(ms^{-1})
Existing sources	Narayan steel	(3000,10000)	374.4	127.6	6.5	100	443.0	5.3
	BASF	(1500,11000)	4.2	0.2	1.5	50	481.0	4.8
	KISCO	(500,7500)	2.2	4.0	3.7	45	443.0	12.0
	KIOCL	(1500,8500)	216.5	82.7	4.0	80	436.0	18.0
	MRPL	(2500,11000)	215.0	106.0	2.8	94	453.0	20.0
Proposed sources	Smith	(0,0)	8.8	81.7	6.0	40	423.0	20.0
	KIOCL extension	(1500,8500)	278.0	36.4	4.0	80	443.0	19.0
	MRPL extension	(2500,11000)	316.0	139.0	2.8	91	473.0	40.0

d_s, H, T_s, V_s represent the internal stack diameter, stack height, stack gas exit temperature and stack gas exit velocity respectively and BASF, KISCO, KIOCL and MRPL represent Badische Aniline-und Soda-Fabrik Company Ltd., Kudremukh Iron & Steel company, Kudremukh Iron & Ore Company Ltd. and Mangalore Refinery Petrochemical Ltd respectively.

χ_i is expressed in terms of the height of inversion layer, Z_i (2.15 σ_{zi}) and σ_{yi} (Stunder and SethuRaman, 1986) as :

$$\chi_i(x,y) = \frac{Q}{\sqrt{2\pi}\, U_s \sigma_{yi} Z_i} \exp\left(-0.5 \frac{y^2}{\sigma_{yi}^2}\right) \tag{11}$$

Maximum concentration (Stunder and SethuRaman, 1986) is obtained along x –axis (y = 0) is given by :

$$\chi_i(x,y) = \frac{Q}{\sqrt{2\pi}\, U_s \sigma_{yi} Z_i} \tag{12}$$

3. Site description and model parameters

Hourly mean values of wind direction (degrees), wind speed (ms^{-1}) and temperature (K) for January, May, July and October of 1996 have been obtained from India Meteorological Department, Panambur station close to the proposed site. Twentyfour hour average GLCs of SO_2 and NO_x have been calculated by ISCST3 model and DDM for the existing and proposed sources in all directions of the site (Fig. 1) at 400 m grid interval during each month. Similar model parameters have been used to calculate 1-hour GLCs of pollutants due to the existing and proposed sources under coastal fumigation. Stack and emission data for SO_2 and NO_x for the existing and proposed major industries in a 10 km radius around the site are given in Table 1.

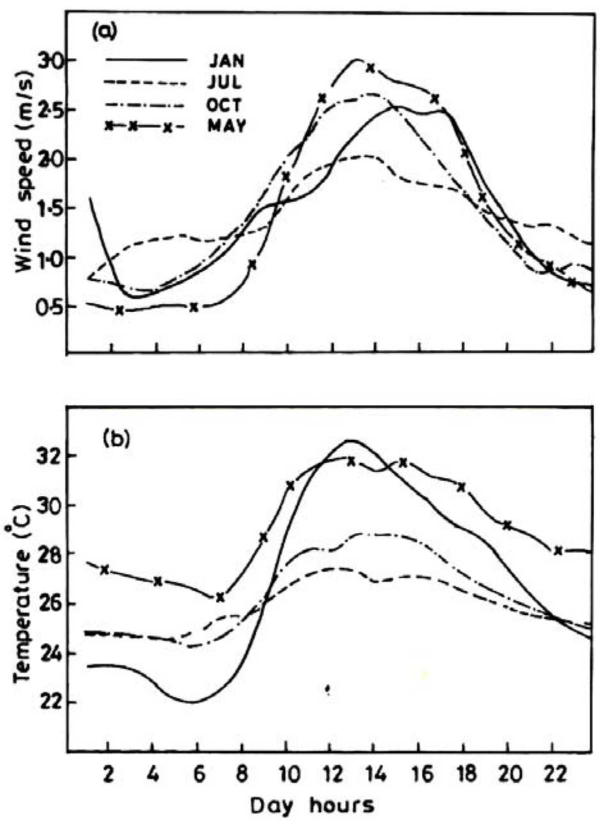

Figs. 2(a&b). Monthly mean values of (a) wind speed and (b) temperature at different hours of the day

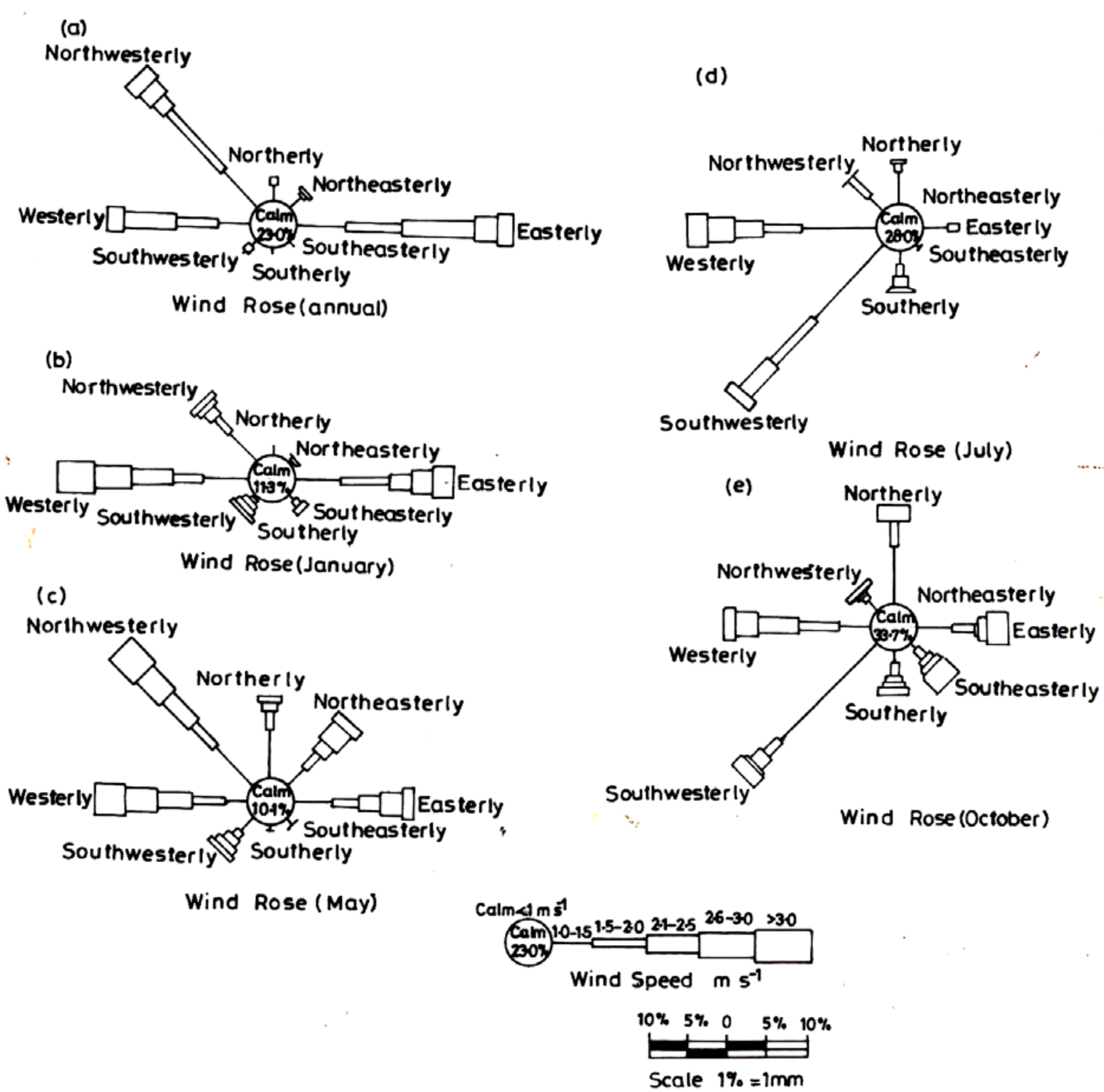

Figs. 3(a-e). Wind roses (a) annual (b) January (c) May (d) July and (e) October. In this figure, the range < 1 ms^{-1} is considered as calm period since the minimum wind speed at stack height is 1 ms^{-1} (U.S. EPA, ISC3, 1995)

Monthly hourly values of wind speed and temperature during January, May, July and October are shown in Figs. 2(a&b). The highest wind speed is observed during May (3.1 ms^{-1}), followed by October (2.7 ms^{-1}), January (2.5 ms^{-1}) and July (2.0 ms^{-1}). The highest temperature was recorded during January (32.3° C), followed by May (32.0° C), October (29.0° C) and July (28.0° C). The annual frequency distribution of the wind directions shows that easterly, westerly or north-westerly are dominant wind fields. These winds fields are dominant during May, January, monsoon and post monsoon periods respectively [Figs. 3(a-e)].

In the absence of on-site data of vertical temperature gradients, median turbulent intensities and wind profile exponents, Pasquill stability categories (Bowers *et al.*, 1979) are appropriate to classify stability since they include wind speed and time of day as well. The 24-hours of the day have been divided into morning, afternoon, evening and night periods. Pasquill stability

TABLE 2

Pasquill stability categories

Time periods	Wind speed (ms^{-1})					
	0-1.5	1.6 - 3.0	3.1 - 5.1	5.2 - 8.2	8.3 - 10.8	>10.8
Night						
Sunset plus 2 hours to sunrise plus 1 hour	E	E	E	D	D	D
Morning						
Sunrise plus 1 hour to sunrise plus 5 hours	C	D	D	D	D	D
Afternoon						
Sunrise plus 5 hours to sunset minus 1 hour	B	B	C	C	D	D
Evening						
Sunset minus 1 hour to sunset plus 2 hour	E	E	D	D	D	D

TABLE 3

24–hr maximum GLCs of SO_2 and NO_x due to the existing industries

Model	Months	SO_2 (μgm^{-3})	Distance (m)	Direction	NO_x (μgm^{-3})	Distance (m)	Direction
ISCST Version 3	January	46.2	9900	South-east	18.7	9900	South-east
	May	78.1	9900	South-east	31.8	9900	South-east
	July	93	9900	South-east	37.4	9900	South-east
	October	74.9	9900	South-east	30.4	9900	South-east
DDM	January	46.6	10400	North-east	17.3	10400	North-east
	May	45.3	4800	South-east	18.4	5200	South-east
	July	52.6	2800	South-east	21	3400	South-east
	October	50.3	9500	South-east	20.9	10200	South-east

categories have been determined on the basis of wind speed and period of the day as given in Table 2. These stability criteria have been used to determine stability classes for the rural area under study. Based on such considerations, the seasonal daily average maximum has been categorized as unstable (stability classes B and C), neutral (D) and stable (E and F). Unstable (B and C) and neutral atmospheric conditions (D) prevail during day hours and stable (E) conditions prevail during night. Diurnal variation of mixing height has been obtained from CPCB (1984-85) as input to the model.

4. Results and discussion

The study employs a workable and easily adaptable procedure to assess 24-hr GLCs of SO_2 and NO_x during January, May, July and October with routine meteorological observations. Model parameters, as stated in Section 3, have been used as input parameters to both dispersion models. It is observed that wind speeds and temperatures over the seasons attain maximum values during the afternoon (1300 – 1500 hr UTC) under unstable and neutral atmospheric conditions. Easterly, westerly or north-westerly winds [Figs. 3(a-e)] are dominant around mid-day as a result of sea and land breeze circulations from and to the Arabian Sea.

4.1. *Existing industrial plants*

The short-term GLCs of SO_2 and NO_x due to the existing pollution sources are calculated by DDM, and results are compared with ISCST3 (Table 3) during each of the months of January, May, July and October. The 24-hr maximum GLCs calculated by ISCST3 model and DDM are observed in the south-east direction of the site during July, which may be the result of dominant, westerly, south-westerly and northerly frequencies as shown in the wind rose [Figs. 3(a-e)]. Further, the predicted SO_2 and NO_x maximum GLCs due to the existing sources may occur during monsoon due to low

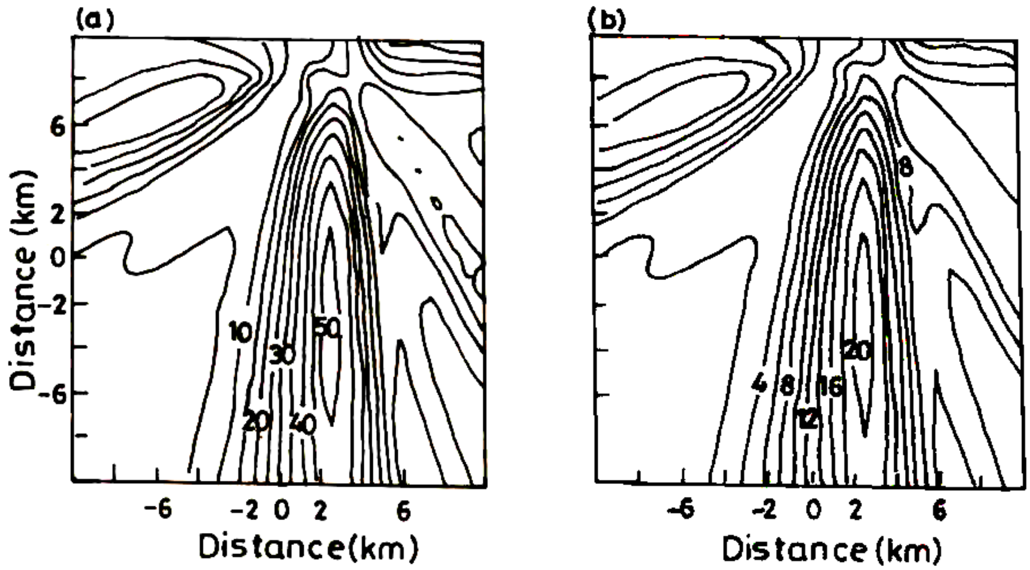

Figs. 4(a&b). 24-hr average GLCs (μgm^{-3}) of (a) SO_2 and (b) NO_x computed by DDM due to the existing pollution sources during monsoon period in the south-east direction of the site. The location of the Tower site is at the coordinate (0,0)

TABLE 4

Comparison of observed concentration with model results (8 hourly average)

Locations	Distance (m) and direction		Observed concentration		Predicted model results			
					DDM		ISCST3	
			SO_2 (μgm^{-3})	NO_x (μgm^{-3})	SO_2 (μgm^{-3})	NO_x (μgm^{-3})	SO_2 (μgm^{-3})	NO_x (μgm^{-3})
Baikampadi	6835,	NNE	7.6	8.8	22.1	9.3	12.3	5.5
Bala	10119,	NNE	6	10.1	15.3	15.7	24.8	12.6
Hosabettu	9732,	NNE	8.3	7.2	26.7	10.4	9.6	3.2
Jokatte	7200,	E	6	8.4	20.3	8.2	50.0	16.9
Kalavar	7353,	NNE	6.4	8.5	19.3	8.3	10.2	5.0
Kolambe	8089,	NNE	6	6.1	17.7	6.9	5.7	1.3
Konchade	2828,	NNE	7.4	5.8	20.2	8.4	13.6	6.7
Kavoor	1200,	E	6.3	8.3	19.8	8.5	2.4	0.9
Panambur	4079,	NNE	7.4	8.2	22.6	8.8	11.7	4.0

wind speeds and temperatures. The deposition of air pollutants at a short distance from the site found by DDM may result due to gravitational settling in the calculation algorithm of GLCs. The short-term SO_2 and NO_x maximum GLCs are found by DDM at a distance of about 3 km, south-east of the site during monsoon period (Table 3).

The combined effect of high wind speed and dominant atmospheric conditions resulted in maximum values of GLCs at long distances during winter and post-monsoon periods. The distribution of SO_2 and NO_x GLCs during monsoon computed by DDM is shown in Figs. 4(a&b). The study has also been extended to estimate short term GLCs on largest human settlements,

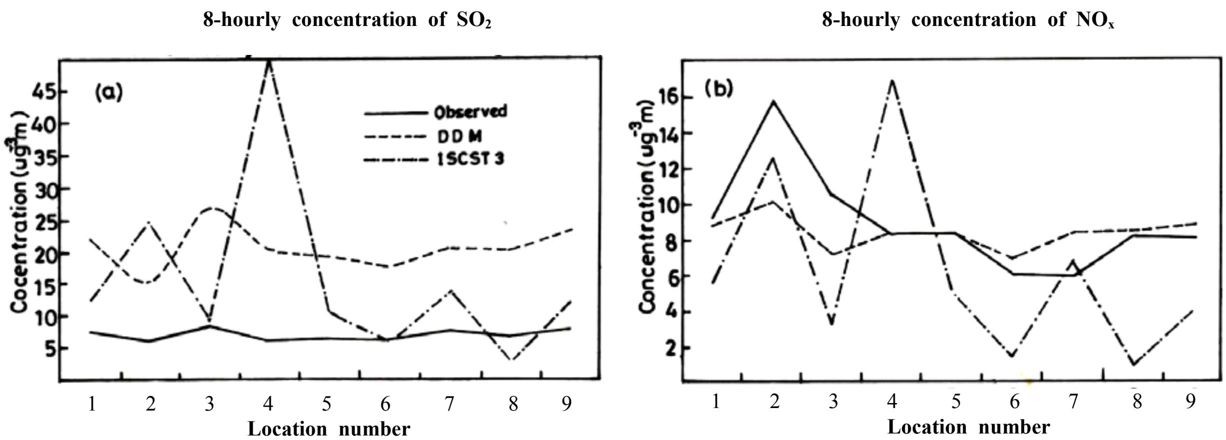

Figs. 5(a&b). Comparison of observed concentrations with model predicted results. Location numbers from 1 to 9 where pollutant concentrations are considered represent the same sites as in Fig. 1

TABLE 5

24-hr maximum GLCs of SO_2 and NO_x due to the proposed industries

Model	Months	SO_2 (μgm^{-3})	Distance (m)	Direction	NO_x (μgm^{-3})	Distance (m)	Direction
ISCST3	January	22.8	9900	South-east	8.7	9900	South-east
	May	37.1	9900	South-east	13.3	9900	South-east
	July	39.1	9900	South-east	13.4	9900	South-east
	October	35.5	9900	South-east	12.9	9900	South-east
DDM	January	28.3	9900	North-east	9.3	6800	South-east
	May	31.5	7400	South-east	12.1	10000	South-east
	July	32.5	5200	South-east	11.9	10000	South-east
	October	38.8	10200	South-east	14	10000	South-east

Mangalore at 2.5 km north-east and Bangare 1 km south of the site (Fig. 1) during January, May, July and October. Short-term GLCs of SO_2 at Mangalore calculated by ISCST3 are 5.8, 19.8, 40.7, 11.8 $\mu g\ m^{-3}$ for January, May, July and October, respectively (Table 6). Similarly the corresponding values obtained at Bangare are 1.5, 2.3, 5.2, 0.3 $\mu g\ m^{-3}$. NO_x are 1.2, 1.8, 5.3, 0.9 $\mu g\ m^{-3}$ and 0.7, 0.9, 3.3, 0.6 $\mu g\ m^{-3}$, respectively. Similar computations are made by DDM. The short-term GLCs of SO_2 computed by DDM are 21.3, 37.3, 47.6, 35.5 $\mu g\ m^{-3}$ and 10.3, 17.9, 24.4, 19.1 $\mu g\ m^{-3}$, and of NO_x 9.3, 15.6, 19.3, 14.3 $\mu g\ m^{-3}$ and 4.4, 7.7, 10.3, 8.0 $\mu g\ m^{-3}$, respectively. High GLCs on human settlements during July may be the result of low wind speed. Predicted SO_2 concentrations by ISCST3 have very high fluctuations at Mangalore in different seasons (Table 6).

The model results are compared with observed 8 hourly average concentrations of pollutants (Table 4) recorded as per the Standards of Central Pollution Board at different locations by West and Gaeke method (1956) for SO_2 and Jacobs and Hochheiser (1958) method for NO_x in the study area during winter by the National Environmental Engineering Research Institute, Nagpur (1993) for the BASF company located within 10 km from the proposed site shown in the Fig. 1. Sulphur dioxide is absorbed by West and Gaeke from air in a solution of sodium or potassium tetra chloromercurate (TCM). This results in formation of dichloro sulphitomercurate complex which resist oxidation by the oxygen in air. Complex is stable to strong oxidants such as ozone and oxides of nitrogen. This solution is treated with solution of sulfamic acid to destroy nitrite anions and then with formaldehyde. The acid bleaches pararosaniline

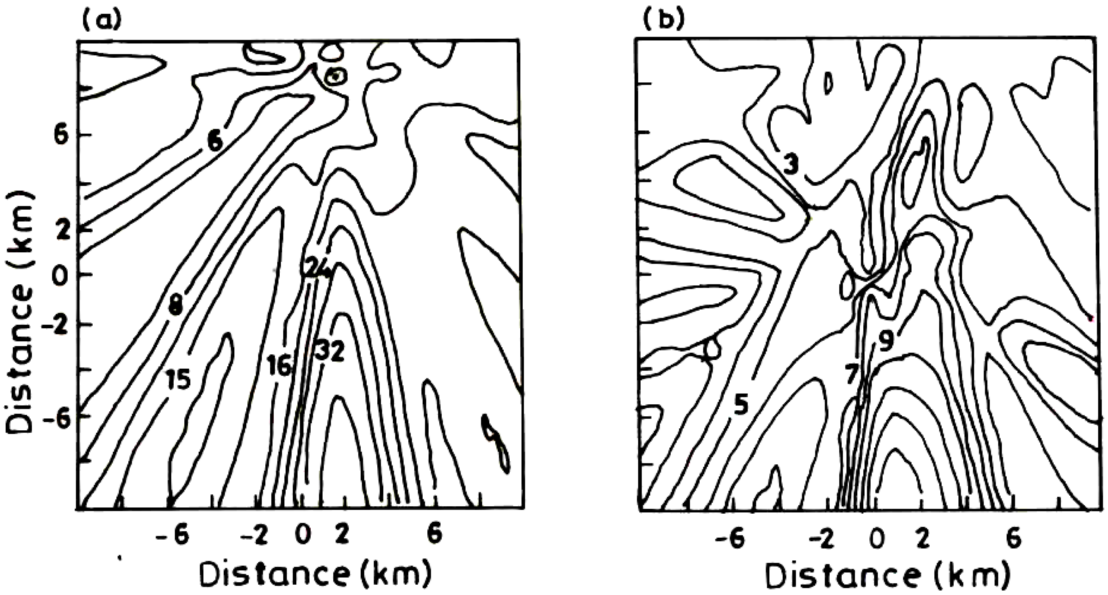

Figs. 6(a&b). Same as in Fig. 4 except for the proposed pollution sources

TABLE 6

24-hr impact of SO_2 and NO_x on largest human settlements

Human settlement	Months	Model	SO_2 (μgm^{-3})	NO_x (μgm^{-3})	Model	SO_2 (μgm^{-3})	NO_x (μgm^{-3})
Mangalore	January	ISCST3	5.1	1.4	DDM	18.2	5.1
	May		11.9	3.4		26	7.9
	July		20.5	4.5		29.4	8.4
	October		7.3	2.6		26	7.4
Bangare	January	ISCST3	1.4	0.5	DDM	10	4.3
	May		3.4	0.8		16.1	6.7
	July		4.5	1.3		19.1	6.9
	October		2.6	0.8		16.7	8.2

containing phosphoric acid. The complex pararosaniline methylesulphonic acid is formed by reaction which is red purple color. Absorbance is measured by spectrophotometer at 560 nm wavelength. This method is implied to get SO_2 concentration in air. Nitrogen oxides are collected by bubbling air through sodium hydroxide solution by Jacobs and Hochheiser method to form sodium nitrite. This involves diazotization of sulphanilic acid by nitrous acid derived from nitrogen oxides followed by a coupling reaction with N (1-naphthyl) ethylenediamine dihydrochloride to form dye. This method was employed to determine NO_x content in the atmosphere. Fig. 5(a) shows 8 hourly average observed concentrations of SO_2 at different locations and the corresponding predicted values by both DDM and ISCST3. Comparison of the three curves in Figs. 5(a&b) indicates that the predicted SO_2 concentrations by ISCST3 are in agreement with the observed concentrations at few locations and are different at these locations in the predicted NO_x levels having very high fluctuations from one location to other with a very large peak at location 4 and a smaller one at location 2. This is unrealistic as compared to the observed values. However, the DDM predicted SO_2 values at almost all the locations have a fixed deviation from the corresponding observed SO_2 concentrations. This deviation is within 2-3 times the

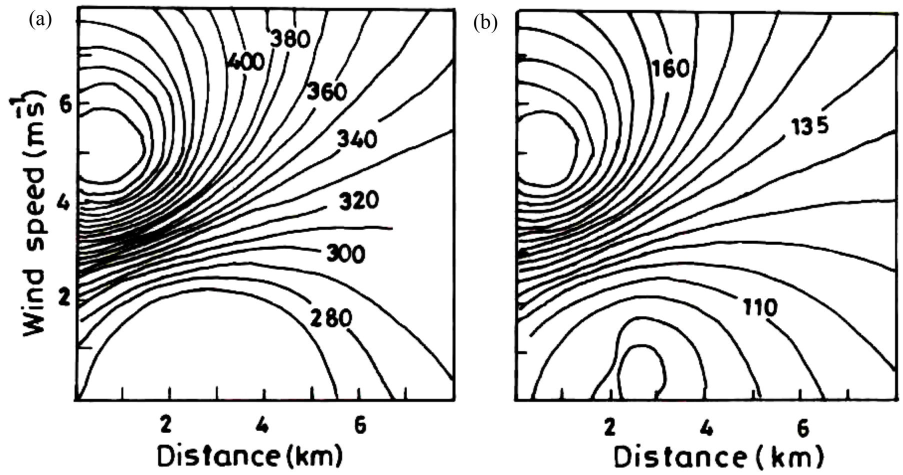

Figs. 7(a&b). 1-hr average GLCs (μgm^{-3}) of (a) SO_2 and (b) NO_x computed under coastal fumigation conditions due to the existing pollution sources during monsoon period. The location of the Tower site is at the coordinate (0,0)

TABLE 7

1-h maximum GLCs of SO_2 and NO_x under Fumigation Condition

Months	SO_2 (μgm^{-3})	Distance (m)	Wind speed (ms^{-1})	NO_x (μgm^{-3})	Distance (m)	Wind speed (ms^{-1})
			Existing industries			
January	495	600	5	195	600	4.7
May	495	600	5	195	600	5.0
July	494	600	4.6	195	600	4.6
October	495	600	4.8	195	600	4.8
			Proposed industries			
January	330	800	5	141	800	50
May	330	800	5	141	800	50
July	321	800	4.6	139	800	4.6
October	348	700	6.2	148	700	6.2

observed values and are accepted as discussed by Singh *et al.* (1990) and Hanna *et al*. (1982). DDM computed values are at 400 m grid and predicted concentration at these locations are the values closest to these grids, where as ISCST3 predicted values are computed on these locations which are at radial distance from the site.

Fig. 5(b) shows 8 hourly average observed NO_x concentrations and the corresponding predicted values by DDM and ISCST3 at different locations. As in Fig. 5(a), the ISCST3 predicted curve has arbitrary fluctuations where as the DDM predicted curve follows the same pattern of the observed values. Unlike the case of SO_2 [Fig. 5(a)], the NO_x predicted concentrations are very close to the corresponding observed values at different locations.

4.2. *Proposed industrial plants*

The short-term GLCs of SO_2 and NO_x due to the proposed pollution sources are calculated by DDM. These results in the study area are compared with ISCST3 values during each of the four months January, May, July and October. The 24-hr maximum GLCs computed by

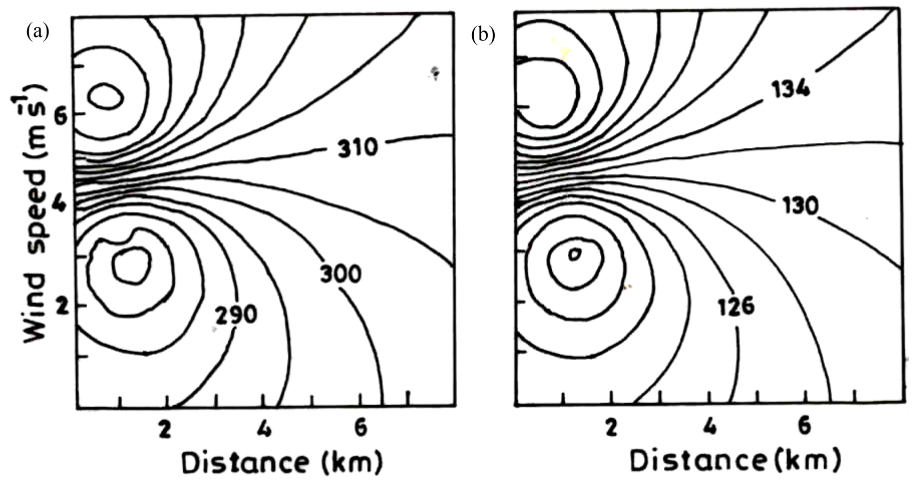

Figs. 8(a&b). Same as in Fig. 7 except for the proposed pollution sources

ISCST3 model and DDM are shown in Table 5. The maximum values are observed in the south-east direction of the site particularly during monsoon, which may be the result of dominant westerly, south-westerly and northerly flows (Fig. 3).

The maximum GLCs of SO_2 and NO_x may occur due to the low wind speeds and temperatures during monsoon period. The combined effect of high wind speed and dominant atmospheric conditions resulted in the maximum value of GLCs at long distances during post-monsoon and winter. The distribution of SO_2 and NO_x GLCs during monsoon computed by DDM is shown in Figs. 6(a&b).

The study has also been extended to estimate short-term GLCs on the large human settlements of Mangalore and Bangare close to the site (Fig. 1) due to the proposed industries during January, May, monsoon and post-monsoon months. Short-term GLCs of SO_2 at Mangalore computed by ISCST3 and DDM (Table 6). High GLCs on human settlement during July may be result of low wind speed.

4.3. *Fumigation conditions*

One hour GLCs of SO_2 and NO_x have been calculated for the existing and proposed pollution sources separately under coastal fumigation during each of the four months of study. The maximum GLC of SO_2 and NO_x is observed at 600 m away from the site under stability class B and wind speed 5 m s^{-1} due to the existing major industries. The maximum GLC of SO_2 and NO_x due to the proposed pollution sources is observed at 700 m from the site under stability class B and wind speed 6.2 m s^{-1} during post-monsoon period, followed by January and May. The least value of GLC is observed during monsoon. One hour GLCs of pollutants due to the existing and proposed industries under coastal fumigation are given in Table 7.

The iso-concentration plots [Figs. 7(a&b)] of pollutants for the selected months show that one - hour GLCs of them are maximum at a distance of 600 m downwind of the site under stability class B and wind speed 5 ms^{-1} due to the existing pollution sources. The maximum GLC of the pollutant due to the proposed industries occurs 700 m downwind under wind speed 6.2 ms^{-1} and stability class B during post-monsoon [Figs. 8(a&b). The occurrence of high GLC is observed during post-monsoon due to the existing and proposed pollution sources for short periods (< 1 hour) and short distances (<1000 m) from the site under wind speeds of 5-6 ms^{-1}.

Wind fields from the north and south are weak. Strong wind fields have been observed from west (Arabian sea) or from east (site and adjoining area of Mangalore city) over the year (Fig. 3). Land and sea breeze features are prominent and can be strong in the early afternoon due to maximization of sea - land temperature difference and high wind speed (6.2 m s^{-1}). This results in maximum GLC under coastal fumigation during post monsoon and January. These results agree with those from an air quality study over Athens basin in Greece (Kambezidis *et al*., 1995 and Kambezidis *et al*., 1998) which shows that the concentration of ozone attains a maximum in the second half of the day during sea-breeze conditions.

5. Conclusions

In this paper, an air quality study has been carried out using a new model named Desein Dipersion Model (DDM) at a coastal region in India. Results obtained from DDM have been compared with those of ISCST version 3 model used by US EPA. The predicted 8 hourly model results of SO_2 and NO_x due to the existing power plants are compared with the observed concentrations at different locations during the same period. Model results show that the predicted SO_2 at almost all the locations by DDM have uniformly higher values from the corresponding observed SO_2 concentrations. This difference is almost constant and is within 2-3 times the observed values which is well accepted as discussed in the literature. On other hand the predicted SO_2 concentrations by ISCST3 have very high fluctuations from one location to the other and this characteristic is unrealistic as compared to the observed values. In case of NO_x, 8 hourly average observed concentrations and the corresponding predicted values by DDM and ISCST3 at different locations show that the ISCST3 predicted curve has arbitrary fluctuations where as the DDM predicted curve follows the same pattern of the observed values. Unlike the case of SO_2, the NO_x predicted concentrations by DDM are very close to the corresponding observed values at different locations.

DDM considers that the air pollutants hit the ground, some of which are deposited permanently and the remainder are reflected. It may be noted that the reflection coefficient is the measure of the pollutants reflected from the ground. DDM has the advantage of including the impact of gravitational settling on the pollutants close to the site. High GLCs of SO_2 and NO_x were predicted due to existing and proposed pollution sources under worst meteorological conditions, and its impact is found to be the highest on human settlements close to the site during monsoon. The impact during May is found to be less than that during monsoon, and it is the least during January. The dominance of westerly, south-westerly and northerly wind directions causes impact of the pollutants at the south-east of the site.

Under coastal fumigation, one hour GLCs of pollutants are higher during post monsoon than in summer. Pollutants generated by industries at coastal region, may be transported under secondary circulation system, caused by land and sea breeze under the influence of strong wind-fields. The monsoon due to its abundant rainfall over India is generally assumed as a very good phenomenon to deposit air pollutants. However, when rainfall is scanty, the strong westerly or north-westerly wind over the site may give rise to high GLCs to the east of the site which is mostly populated. The results have interesting implications and need further investigations.

Acknowledgements

The observed Ambient Air Quality data used in the study have been taken from National Environmental Engineering Research Institute, Nagpur, India and the meteorological data used in the study have been obtained from the India Meteorological Department. The rest of the data used are collected by Environment Management Division, Desein Pvt. Ltd., GK-II, New Delhi, India.

References

Bower, J. S., Broughton, G. F., Stedman, J. R. and William, M. L., 1994, "A winter NO_2 smoge episode in U.K.", *Atmospheric Environment*, **28**, 3, 461-475.

Bowers, J. F, Bjorkland, J. R. and Cheney, C. S., 1979, "Industrial source complex (ISC) dispersion model", US Environment Protection Agency report, EPA-450.

Carrol, J. J. and Baskett, R. L., 1979, "Dependence of air quality in a remote location on local and mesoscale transports, A case study", *J. Applied Meteorology*, **18**, 474-486.

Central Pollution Control Board, New Delhi, Publication, 1997-98, "Assessment of Impact to Air Environment : Guide line to conducting Air Quality Modelling", PROBES 70.

Central Pollution Control Board, New Delhi, Publication, 1984-85, "Control of urban pollution series", CUPS 13.

Dumbauld, R. K., Rafferty, J. E. and Cramer, H. E., 1976, "Dispersion deposition from aerial spray release", Third symposium on atmospheric diffusion and air quality, *American Meteorological Society*, Boston.

Hanna, S. R., Briggs, G. A. and Hosker, R. P., 1982, "Hand book on Atmospheric Diffusion", ARDL NOAA, USA, Tech. Information Centre No. 11223, U.S. Department of Energy.

Jacobs, M. B. and Hochheiser, S., 1958, "Continuous sampling and ultra micro determination of Nitrogen Oxide in Air", *Anal., Chem*., **30**, p426.

Kambezidis, H. D., Peppes, A. A. and Melas, D., 1995, "An Environmental experiments over Athens urban area under sea – breeze conditions", *Atmospheric Research*, **36**, 139-156.

Kambezidis, H. D., Weidauer, D., Metas, D. and Ulbricht, M., 1998, "Air Quality in the Athens Basin during sea-breeze and non-sea breeze days using laser-remote sensing technique", *Atmospheric Environment*, **32**, p12.

Khemani, L., Monin, T., Prakasa, G. A., Safai, P. S., Singh, P. D., Chaterjee, G. R. N. and Prakash, P., 1989, "Long term effects of air pollutants on pH of rain water in north India", *Atmospheric Environment*, **23A**, p753.

Kurita, H., Ueda, H. and Mitsumoto, S., 1990, "Combination of local wind system under gradient wind condition and its contribution to the long range transport of air pollution", *J. Applied Meteorology*, **29**, 331-348.

Lu, R. and Turco, R. P., 1994, "Air pollutant transport in coastal environment, Part–I, Two dimensional simulations of sea - breeze and mountain effects", *J. Atmospheric Science*, **51**, 2285-2308.

Lu, R. and Turco, R. P., 1995, "Air pollutant transport in coastal environment, Part -II, Three dimensional simulations over Los Angels, Basin", *Atmospheric Environment*, **29**, 1483-1599.

National Environmental Engineering Research Institute, 1993, "Environmental Impact Assessment of Chemical Complex of BASF India Limited", Mangalore.

Robert, J. U., 1990, "The atmospheric chemistry of organic nitrates", *Atmospheric Environment*, **24A**, 243-287.

Savijarvi, H., 1995, "Sea breeze effects on large scale atmospheric flow", *Beitr. Phys., Atmos*., **68**, 335-344.

Simpson, J. A., 1994, "Sea-Breeze and local winds", Cambridge University press, p234.

Singh, M. P., Goel, P., Panwar, P. S., Agarwal, P., Nigam, S. and Bagchi, N., 1990, "Predicted and observed concentration of SO_2", SPM and NO_x over Delhi, *Atmospheric Environment*, **24A**, 783-788.

Stunder, M. and SethuRaman, S., 1986, "A statistical evaluation and comparison of coastal point source dispersion models", *Atmospheric Environment*, **20**, 301-315.

U.S. Environmental Protection Agency, 1995, "Industrial Source Complex (ISC3) Dispersion Model".

Wakimoto, R. M. and McElory, J. L., 1986, "Lidar observation of elevated pollution layers over Los Angles", *J. Climate, Applied Meteorology*, **25**, 1583-1599.

West, P. W. and Gaeke, C. C., 1956, "Fixation of Sulphur Oxide as Sulfitomercurate III and subsequent colorimetric determination", *Anal., Chem*., **28**, 1816.